Thermoacoustic analysis of the dynamic pressure inside a model combustor during limit cycle oscillations

Panduranga Reddy Alemela*, Juan Roman Casado, Santosh Kumar and Jim Kok

Laboratory of Thermal Engineering, University of Twente, Netherlands

[Received date August 8, 2012; Revised version received on January 28, 2013; Accepted date: February 04, 2013]

ABSTRACT

In this work comprehensive experimental and numerical studies incorporating the most relevant physical mechanisms causing limit cycle pressure and combustion rate oscillations (LCO) in a laboratory scale combustor will be discussed. The strong interaction between the aerodynamics-combustion-acoustic oscillations (ACA), and under specific conditions the aerodynamics-combustion-structural vibrations (ACS), is studied by a careful selection of experiments and numerical simulations performed using commercially available computational models. It is shown predominantly that the convective time scales due to the aerodynamics at the flame stabilizer and the time period related to acoustic propagation have to be of the same order in magnitude to be able to drive the system into LCO. The measurements indicated that the frequency spectrum of the oscillations of the LCO has a distinct peak close to the natural mode of the combustor along with higher order "harmonics" due to non-linear effects. Some non-harmonic higher order peaks are observed that are associated with the structural (liner) natural frequencies of vibration. A numerical simulation has been performed using the commercial code (ANSYS V13.0) that includes the effects of fluid-structure interaction by means of pressure load transfer on to the structure and vice-versa. The fluid domain is modeled using CFX and the structural domain is represented by ANSYS. The information is exchanged between the two domains dynamically at every time step computed. In order to reduce the computational effort and quickly gain insight into the problem only a 2 mm slice of the whole geometry has been considered making it essentially a 2D analysis. The good agreement between the model and measured instability frequencies shows a very promising approach in predicting the limit cycle oscillations in this kind of configurations.

Keywords: Thermoacoustics, limit cycle oscillations, CFD, fluid structure interaction

*Correspondence email-address: pandu.alemela@gmail.com

1. INTRODUCTION

Stringent emission control policies adapted by various governments in the recent past have lead the industries in the energy sector to design and develop more eco-friendly and efficient combustion systems. Lean premixed combustion (LP) technology is one among the promising solutions that can assure low (NO_x) emissions [1, 2]. However, these new technologies are associated with flame stability issues well known as thermoacoustic instabilities. Here the aerodynamics-combustion-acoustics (ACA) feedback loop, present in the combustor (see Figure 1a) can cause the pressure inside the combustor to grow into limit cycle oscillations of pressure and heat release rate (LCO) [3]. Several papers in literature, showing different mechanisms responsible for such feedback loop to occur and eventually turn into LCO, have been published [4]–[13]. As an example, the work performed by Chakravarthy et al. [9] can be considered to understand the most relevant feedback loop mechanisms possible. This is similar to the current configuration with a non-premixed flame stabilised in a shear layer, but due to back ward facing step. However, their global equivalence ratio (ϕ = 0.03 to 0.13) indicated, is an order of magnitude less than the practical flame applications like in the Gas Turbine conditions (ϕ~0.4). They observed, with an increase in flow velocity (towards high Re), the dominant frequency (flow-acoustic lock on frequency) does not change, as opposed to what should be expected corresponding to the frequency of a vortex shedding mechanism. This is very well explained in terms of dimensionless numbers Strouhal (flow instabilities) and Helmholtz number (duct acoustic processes) separating these two mechanisms. They pointed out that the shear layer oscillations modulate the heat release fluctuations that are the source of acoustic oscillations, and the frequency of the former matches with one of the natural acoustic modes of the duct, thus forming a resonance between both the processes. A remarkable finding is that the peak amplitude shows a non-linear increasing trend at the lock-on frequency. In the works of Fureby et al. [10], with Reynolds numbers similar to the present study, they suggest that the strength of the large vortices, which appeared in cold flow, is decreased in the reacting case as a result of the change in the viscosity, which decreases the Reynolds Number. But such stabilizing effects occur only at high Reynolds numbers and are greatly influenced by the blockage effects. Fureby et al. [11]

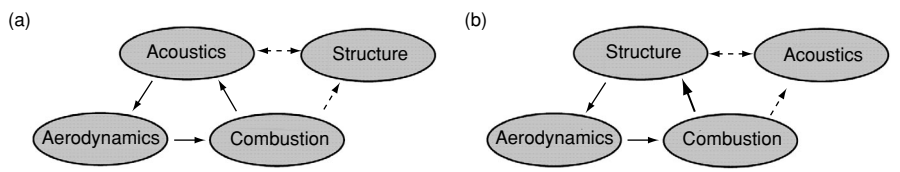

Figure 1: (a). Schematic of the Aerodynamics – Combustion – Acoustics (ACA) feed back loop mechanism, where the structure may play only a passive role (1-way interaction). (b). Aerodynamics – Combustion – Structure (ACS) feed back loop mechanism, where the acoustics plays a passive role and instead the structure plays a strong active role (2-way interaction).

have also performed LES on a similar test case and suggested that the frequency of vortex shedding in the reacting case has shifted from 100 Hz in cold case to 120 Hz characterized by periodic vortex shedding from both sides of the bluff body. Most of the above works were made using gaseous fuel and using linear stability models, mainly aiming at gas turbine applications. However, Mariappan and Sujith [13] have performed an analytical investigation, to understand and predict the thermoacoustic instability in solid rocket motors, taking into account the non-orthoganality of the eigen modes of the system with strong coupling between the acoustic field and propellant burn rate. Unlike the classical linear stability predictions, which are valid in the large time limit, they proposed a generalised stability theory, including the non-linearities, valid for all times i.e., which measures the growth as well as the decay rate of the oscillations. This approach has been further applied also to ducted premixed and diffusion flames [14].

It can be summarised from the above literature work that only those time scales of convective transport, that are of the same order in magnitude of the acoustic time period of the natural modes in the combustor, will couple strongly and provide strong feed back to develop further into a LCO. However, this may be true depending on a specific geometry/configuration and subjected to acoustic energy losses through the boundaries i.e., at various inlets, outlets, structural walls (liners) etc.. In most of the above cases mentioned from the literature, the combustor walls/structure remains passive and does not play any role in the feedback loop (thus has a very weak influence on the Rayleigh criteria). On the other hand, in the combustion systems with relatively thin flexible walls (e.g., the GT combustor liner) there can be a strong interaction between the aerodynamics-combustion-structure (ACS). Here the structure can play an active role in the formation of LCO behaviour (see Figure 1b). This mechanism is relatively new and only a few publications are available in literature [15]–[19]. Depending on how and to what extent the combustion noise (broad band noise) gets coupled with the structural natural modes, this new alternative feedback loop mechanism (ACS) can bring the system into LCO. This may induce large amplitude vibrations of the liner structure and might even lead to failure of the component as reported by Tinga et al. [16]. To understand and capture this entire set of phenomenon interacting together, different numerical approaches were developed by Pozarlik et al. [17] and Huls [18]. CFD is used for fluid domain and FEM is used for structural domain and both were coupled together directly in Fluid Structure Interaction (FSI) and indirectly in Acousto-Elastic analysis. The developed tools were validated with the experimental results with limited success in predicting the dangerous frequencies but not the amplitudes and their growth rates. Due to the multi-disciplinary nature of the problem, and complexity involved in various interactions/modes, there is still a considerable gap in thorough understanding and modelling capabilities of all the responsible mechanisms that lead to the LCO applicable in general to any combustion system.

In the present work, an attempt has been made to include the relatively new feedback mechanism ACS that might lead and/or contribute to formation of LCO along with the classical ACA mechanism. A numerical simulation has been performed with coupled fluid-structure (2-way) interaction using commercially available software (ANSYS-workbench V13) and has been verified with few experimental observations [19].

2. EXPERIMENTAL AND NUMERICAL SETUP

A schematic view (left side) and the actual picture (right) of the LIMOUSINE model combustor used for this investigation are shown in Figure 2. The setup is made essentially to represent a Rijke tube combustor [20] with air injected uniformly from the bottom side and the fuel as methane gas is injected along the triangular wedge located at about one third of the height of the duct. The upstream duct is made of 25 × 150 mm^2 cross-section, whereas the downstream duct has a 50 × 150 mm^2 cross-section to compensate the volume expansion due to combustion. Two configurations were investigated: single (short) and the double (long) liner configuration. The main difference between these two configurations is that an additional duct of length 620 mm is mounted on the single liner setup (see Figure 2, left), making it a double liner configuration (see Figure 2, center). By this way we can vary the longitudinal resonance modes (frequency and there by acoustic time periods) by changing the geometric length of the combustor.

The locations of various used instruments to measure the dynamic pressure, temperature, Laser Doppler Vibrometer (LDV), and OH*- chemiluminescence release from the flame with a Photo Multiplier Tube, are shown in the figure. This modular combustor has optical accessibility in all four directions for using advanced laser based

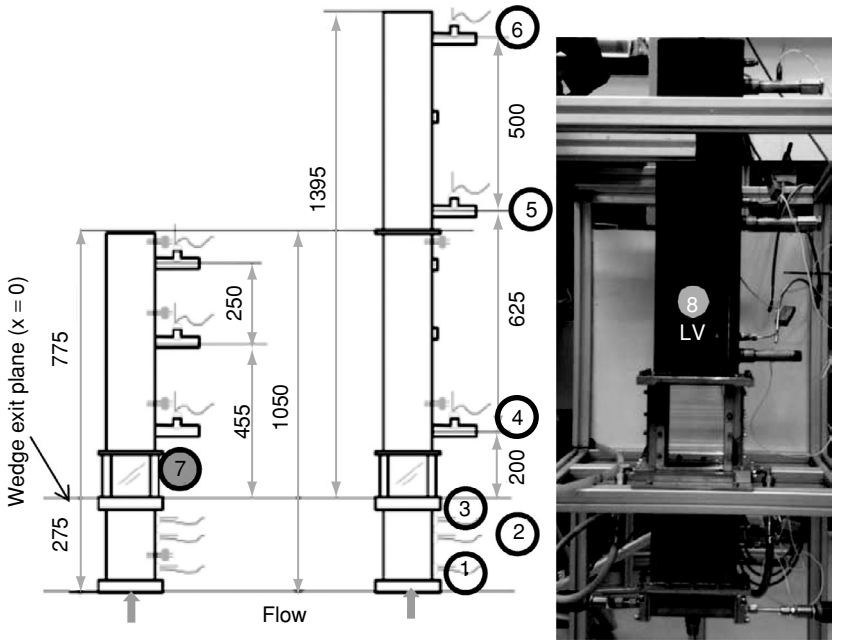

Figure 2: A schematic view of the single (left) and double (centre) liner configuration of the LIMOUSINE model combustor (right). The axial microphone (1–6), UV-PMT (7) and the Laser Doppler Vibrometer (8) locations are also indicated in the schematic.

techniques like PIV and high speed CCD imaging. Special care has been taken to provide an acoustically closed end boundary condition at the air and fuel supply lines by means of choked nozzles. More details on this setup can be obtained from a previous publication by the authors [21].

Using the multi microphone method (*MMM*) in a case without flow or combustion [22], the reflection coefficient R has been obtained at both ends [23]. Here a row of microphones placed upstream and downstream of the wedge measures the dynamic pressure provided by a speaker excitation at several frequencies. A wave field is reconstructed from the measured complex pressure amplitudes in terms of forward (f) and backward (g) travelling waves (Riemann invariants) f and g's. The ratio of these waves gives the reflection coefficient $R = g/f$ in a chosen reference plane. The other advantage of using *MMM* (also in case of flow and combustion) is that we can obtain the acoustic velocity fluctuations, in any given plane by just measuring the acoustic pressure field. Otherwise it is very difficult to measure this, using fragile hot wire probes in the presence of combustion. This is a very important feature of the setup for further thermoacoustic studies performed involving flame transfer (or describing) function measurements.

The numerical simulations were made using ANSYS workbench V13. The idea is to use the existing commercial package, which includes the fluid structure interaction. It focuses on the simplicity of the 2D modeling efforts on these kinds of geometries before going to heavy computational efforts. This model gives some basic understanding of the thermoacoustic phenomenon in a simple configuration and is further useful to reveal the complex interaction between the thermoacoustic oscillations and the structural vibrations [19]. Here the wall pressure loads as computed in the CFD domain, were transferred on to the structural domain and vice versa, making it a coupled (2-way) fluid-structure interaction simulation. This was done fairly easy, compared to the previous investigations where additional interface software (MFX) between the CFD and structural domains was required with relatively long computational times [17],[18]. A schematic of the numerical setup, geometry and model details used in the present work are shown in Figure 3.

For the fluid domain simulation, the SAS-SST turbulence model and the pdf-flamelet combustion model were used. For more details on the model implementation see [19]. A total physical time of 0.5 s with time steps (Δt) of 0.0001 s and target residual value of 0.0001 has been used. The transient data is stored for every 10^{th} time step giving flow data available at a "sampling" frequency of 1000 Hz. This allows analyzing the data up to 500 Hz according to the Nyquist criterion. The mesh quality as indicated by the CFL number ($C = U^*\Delta t/\Delta x$) for this configuration is calculated to be around 1. The combustor boundary conditions were chosen as follows: At the air and fuel inlet: normal speed calculated on basis of the mass flow and outlet: the average static pressure 0 [Pa] was imposed. This configuration is observed to be acting like an acoustically closed-open type boundary condition, which is a variation of a simple Rijke tube but with the upstream end closed. Therefore classical analytical solutions, for the acoustic oscillations in the duct, can still be used for the frequency analysis.

	Model
Turbulence	SAS-SST
Combustion	PDF-flamelet

	Upstream (m)	Down-stream (m)
Length	0.220	0.780
Width	0.025	0.050
Wall thickness	0.004	
Wedge	0.024	

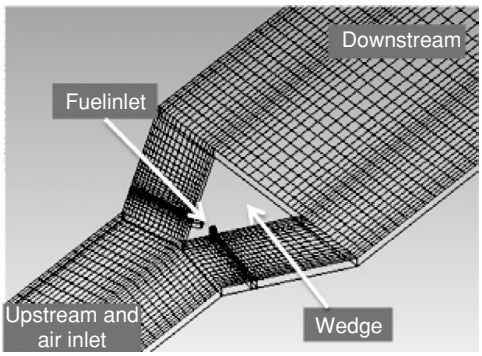

Figure 3: Schematic of the geometry, model details and numerical setup used for Limousine combustor.

For the structural domain simulation, the material element type (ET) SHELL63 with wall thickness of 4 mm and at a constant temperature of 400°C (Young's Elastic Modulus (EX): 1.76E11N/m^2) has been used. Only the structure downstream of the wedge is considered for the transient structural analysis. This is because most of the dynamic coupling between the hot fluid and structure occurs in the downstream region of the wedge. Conform to the experimental setup, the clamped boundary conditions with constraints at selected nodes axially, i.e., at Z = 0 and 0.760 m were implemented. The rest of the surface is free to deform depending on the dynamic pressure loads.

3. RESULTS AND DISCUSSIONS

3.1. Acoustic boundary conditions and operating domain

First we will present the measured cold acoustic boundary conditions at the inlet and exit of the setup. Using the Multi Microphone Method (*MMM*) [22] the reflection coefficient, *R* has been obtained at both ends [23] as shown in Figure 4. The set up in the present configuration acts like a Rijke tube, but with one end closed at the inlet and the other as open end at the exit. This is confirmed by a comparison of acoustic theory predictions and measured values of *R* about 1 and –1 in real and phase values of 0 and $-\pi$ at the closed and open end respectively. In both the single and double liner configuration the acoustic end boundary conditions were measured to be identical. This was to be expected, as they do not depend on the length of the combustor.

With the above boundary conditions (assuming they are not changed by flow or temperature increase due to combustion), the first natural mode acoustic eigen frequencies of the combustor can be calculated at the combustion conditions from the simple duct correlation $(2n–1)/c/4/L$ with n = 1,2,3... These are calculated to be around 178 Hz and 106 Hz in single and double liner configuration with a length averaged temperature of the combustor around 1250 K and assuming the gas speed of sound to be given by the expression for a perfect gas. The dynamic pressure measurements made in the double liner configuration with a flame showed a distinct peak frequency around the first Eigen mode of the combustor for several operating points with varying thermal

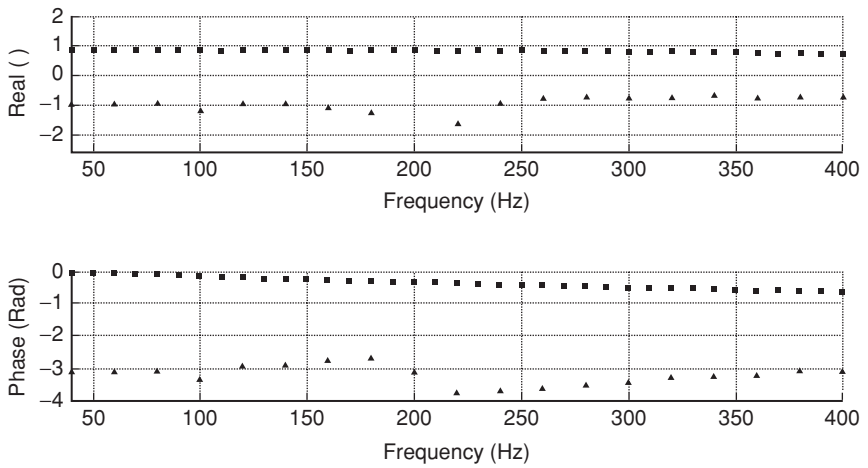

Figure 4: The real values and phase angle of the measured reflection coefficient as a function of frequency at the upstream (squares) and downstream (triangles) end of the model combustor. The values indicate an acoustically closed end and open end at upstream and downstream side respectively.

power and air excess ratio. The results are shown in Table 1. It can be noted that the peak frequency (4th column) is weakly dependent on the flow rates, increasing with thermal power and air excess factor, represented by Reynolds number (*Re*) based on the

Table 1: Measured peak frequencies, amplitudes and temperatures in the combustor during several operating points (characterized by Th. Power [kW], air excess factor [λ] and Reynolds number, Re based on wedge size), in the double liner configuration (*L* = 1.67 m). Peak amplitudes and frequencies are taken from microphone location 1 at x = –179 mm upstream of the triangular wedge

Th. Power [kW]	Air factor λ [–]	Re [–]	Peak Freq. [Hz]	Mic 1 Amp. [Pa]	Temp. in Comb. [°C]
40	1.4	5597	102.65	18.9332	839
40	1.6	6364	100.465	32.6326	945
50	1.4	6996	102.345	42.3696	985
50	1.6	7955	104.745	77.9246	947
60	1.4	8395	102.05	74.919	1045
60	1.6	9547	109.545	1384.89	963
60	1.8	10698	110.005	1830.79	900
60	2	11849	110.31	1671.02	900
60	2.2	13000	110.31	1643.33	900

side of the triangular wedge size (22 mm). This can be attributed to a change of heat losses at different operating points, which influences the average speed of sound inside the combustor. However, the measured peak amplitude is strongly influenced by the mean flow field, which will be discussed in the follow-up sections.

The above analysis is used to verify the mode shape obtained from the pressure measurements at various axial locations (1–6) as shown in Figure 5. The mode shape is obtained using the peak amplitude and phase values belonging to the first peak

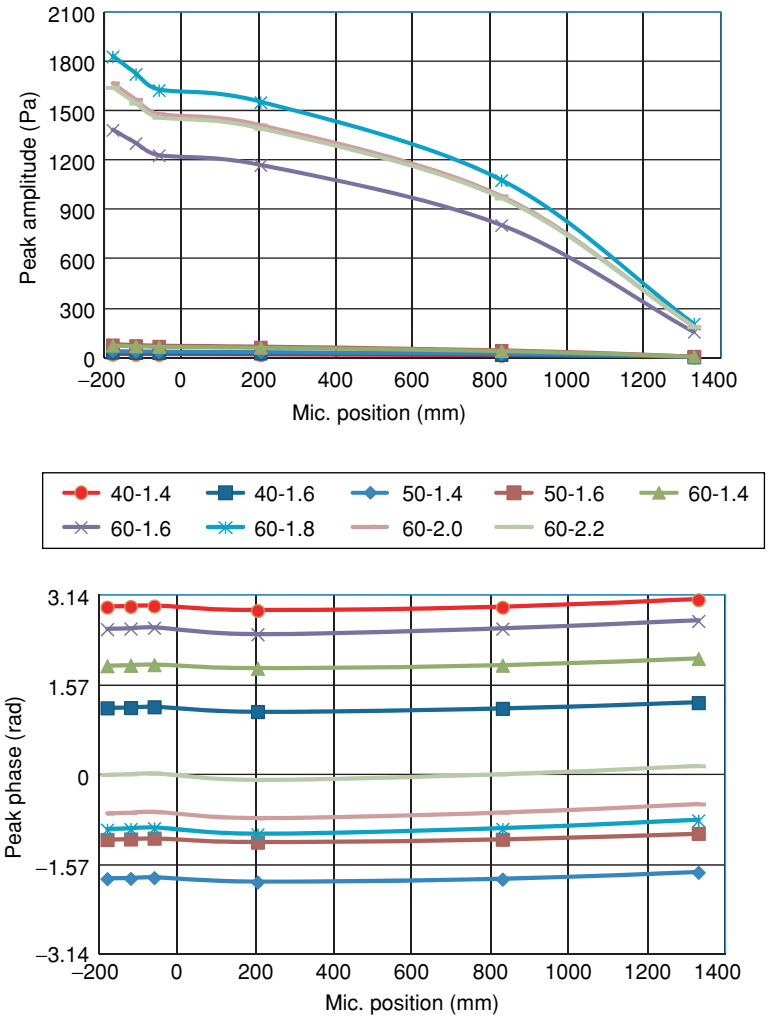

Figure 5: The first Eigen mode shape obtained from the measured peak amplitude (a) and phase (b) along several axial locations. The mode shape indicates the typical quarter wave mode in a simple duct with acoustically closed-open ends.

frequency measured in the combustor and plotted along the combustor. The mode shape measured typically characterizes a quarter wave mode (standing wave, with constant phase) inside a simple duct with maximum pressure amplitude (anti-node) towards the closed end and minimum pressure amplitude (node) towards the open end. This behavior of the setup was very well reproducible at several operating points. Even at the lower flow rates (e.g. 40 kW and 50 kW cases), the pressure oscillation profile was typical for a quarter wavelength standing wave. Even though the amplitudes were an order of magnitude lower, this was very much clear from the constant phase measured axially, which is typical for a standing wave pattern.

3.2. Limit cycle oscillations (LCO)

The measured dynamic pressure time trace in [Pa] and its frequency spectrum [SPL in dB, with reference pressure of 20 μPa), at a location 205 mm downstream of the wedge, are shown in Figure 6 and Figure 7. In the **single liner** (short combustor, 1 m long) configuration, there were no Limit Cycle Oscillations observed (see Figure 6). It was understood from the experimental observations that the flame is very long due to partial (improper) mixing of the fuel with the air. This was measured by the OH*-chemiluminescence images obtained at 500 Hz by a CCD camera mounted with a band pass filter (peaking around 308 nm). It can be argued that the OH*-chemiluminescence signal captured by the camera may not be actual representative of the location of maximum heat release [24] (flame length, X_{OH*max}) as in this case it is not a perfectly

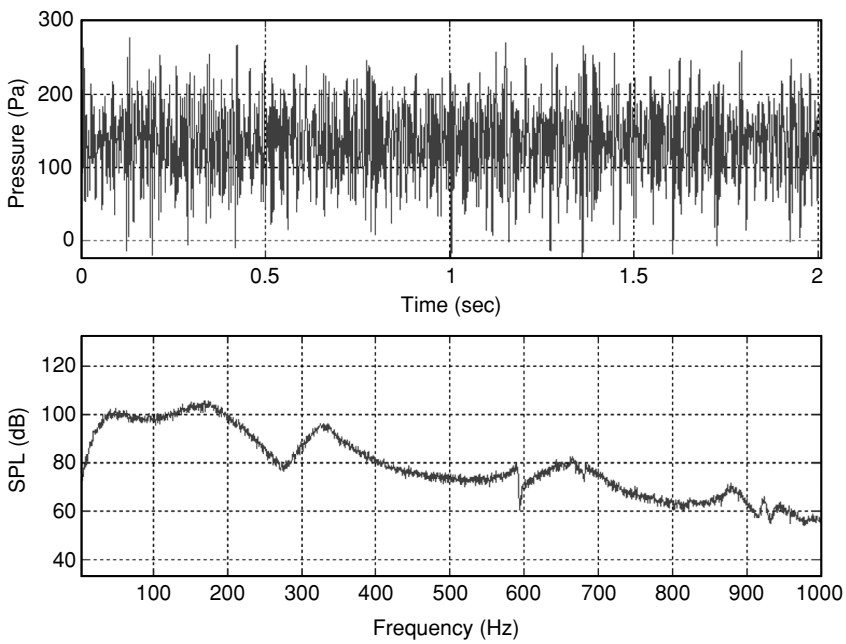

Figure 6: Time domain [Pa] and auto spectrum [SPL, dB] of the pressure signal at 60 kW and λ = 1.60 with single liner. No LCO are observed.

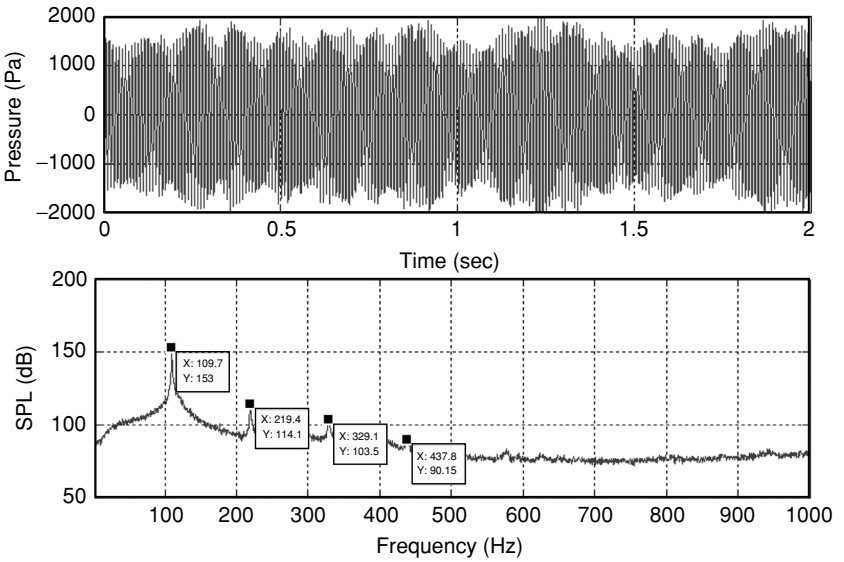

Figure 7: Time domain [Pa] and auto spectrum [SPL, dB] of the pressure signal at 60 kW and $\lambda = 1.60$ with double liner. LCO with distinct peak frequency can be observed.

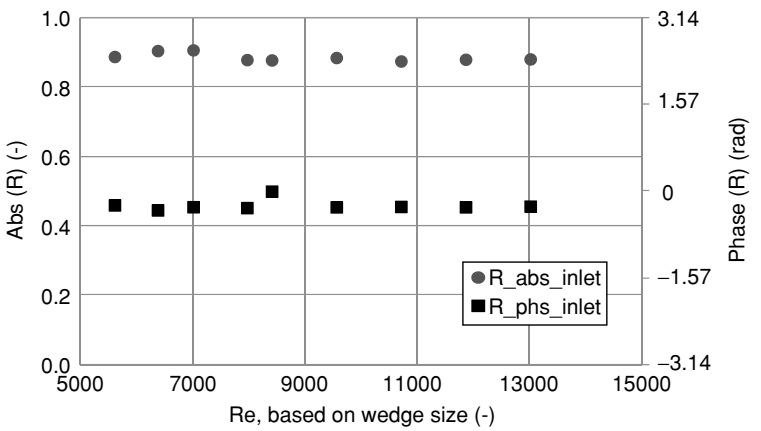

Figure 8: Measured Reflection coefficient absolute and phase values in the air inlet plane (upstream end), corresponding to the LCO frequencies, as a function of flow rates.

premixed flame. However for a qualitative treatment these measurements would be sufficient to characterize the flame and its stabilization behavior. The convective time scale (τ_{conv}) is defined as the time required for any perturbations in the flow at the point

of fuel injection to travel to the location of the flame (X_{OH^*max}) with effective mean convective speed (U_{eff}) [25]. This can be represented mathematically as

$$\tau_{conv} \sim X_{OH^*max} / U_{eff} \tag{1}$$

For the case of 60 kW and air excess ratio (λ) of 1.6 the U_{eff} = 8 m/s and X_{OH^*max} ~ 100 mm, we get a τ_{conv} equal to 12.5 ms. From simple duct analysis the acoustic standing wave time period corresponding to this geometry with closed-open end conditions we calculate the first eigen mode frequency f_1 to be 180 Hz ($f_n = (2n-1)c/4/L$, with average speed of sound in the combustor equal to 720 m/s, L = 1 m). This gives us the acoustic time period ($T = 1/f_1$) of this mode as 5.5 ms. This value is a factor 2.3 smaller as compared to the convective time scale as obtained earlier. According to Lieuwen et al. [4] & [8] there can be an active feedback loop between the flame and acoustics in a combustor only in case the convective time scales are of the same order of magnitude as one of the acoustic mode time period. This is represented mathematically as

$$C - \frac{1}{4} < n.\tau_{conv} \Big/ T < C + \frac{1}{4} \tag{2}$$

Where C~1 is a constant depending on the type of boundary/fuel end conditions and n is an integer with, n = 1,2,3.... Although, from Figure 6, modest amplitude maximum can be observed in the SPL plot around 180 Hz, the feedback is not strong enough to bring the combustor into LCO. From the above analysis we see that the $\tau_{conv} \sim 2.3T$, therefore it can be concluded that significant feedback between the pressure and flame was not possible and hence a LCO has not been achieved in this configuration, for all the operating points investigated.

Whereas in the **double liner** (L = 1.67 m) configuration, for the same operation point (60 kW, λ = 1.60) with almost the same flame stabilization characteristics we get the τ_{conv} ~ 12.5 ms. However, the acoustic time period (T) in this configuration will be 9.3 ms (with c = 720 m/s and f_1 = 108 Hz). Now comparing with Eqn. 2, we get τ_{conv} ~ 1.3 T, which closely satisfies the relation to provide the significant feedback between the flame and the acoustics in the chamber. Thus, in the double liner configuration the LCO is expected to develop and was indeed observed. The LCO was observed to be even more prominent at higher flow rates, as this reduces the convective time scales further ($\tau_{conv} \sim T$). It is observed there is a negligible influence of the flow rates on the frequency of the LCO. However, the amplitude of the LCO increased with the flow rates very significantly. Care should be taken while interpreting these results based on the equation (2) presented above. Because this is one of the many feedback processes that can induce the instability. More important is that the acoustic energy, accumulated due to the feedback process, should be greater than the acoustic losses within the system to bring the system into LCO. Once the system reaches the LCO, a non-linear saturation mechanism [26] will reduce the feedback rate and the LCO will reach constant finite amplitude as shown in Figure 7.

In the **double liner** configuration thus it can be concluded that there is a "match" of the convective time scales and the acoustic time period and that this results in development of the LCO. The second and higher "harmonics" due to non-linear effects during the LCO can be observed from the plot. As can be seen they correspond exactly to the integer multiples of the fundamental mode ($f = n.f_1$). i.e., (f = 109.7, 219.4, 329.1, 437.8...nf_1 Hz, with n = 1, 2, 3, 4…). This is a classical example of the non-linearities in the heat release term, which cause the frequency doubling in the pressure oscillations [27]. Later, with a small change in the burner geometry (the reduced burner exit area, not considered in this frame work), leading to a shorter flame, the LCO was observed even in the **single liner** combustor. It could be explained by the fact that the convective time scale had been reduced due to improved mixing and is now "matching" the acoustic time period. Therefore an active feedback loop is formed between the flame and the acoustics in the chamber resulting in the LCO. These results from the authors will be discussed in detail in a follow up paper.

On the other hand, the LCO amplitudes and frequencies do also depend on the type of acoustic end boundary conditions the flow field experiences in the presence of mean flow and combustion. Lamraoui et al. [29], calculated peak frequencies using a two-coupled-cavity model with a realistic impedance of the system at pre-mixer inlet. In particular, by using the measured phase value of the R as the pre-mixer inlet boundary condition, they predicted very well the measured non-harmonic peak frequencies during the LCO. This motivated the authors to check if the measured R amplitudes and phase values during the LCO (with mean flow and combustion) are identical to those in the case without mean flow as presented previously in Figure 4. The R coefficients measured during the LCO are plotted as a function of flow rates. They show an approximately constant behavior with absolute values around 0.9 and phase values about –0.3 radians. Hence they behave similar to an acoustically closed end boundary condition, independent of flow rates in this geometric configuration. This can also be deduced from the weak dependency of the LCO frequency on flow rates, unlike as reported by Lamraoui et al. [29] and Chakravarthy et al. [9].

Further analysis is carried out to address the behavior of measured amplitudes and frequencies during the presence of LCO. As motivated from the previous investigations [9], the measured frequencies are dependent on dimensionless numbers such as the Helmholtz number ($He = f.L/c$) and the Strouhal number ($Str = f.D/U$) as a function of the Reynolds number (Re) based on a wedge size (22 mm). The variations in He and Str are used to characterize the measured frequencies of the LCO as corresponding to the natural acoustic modes or vortex shedding process. As shown in Figure 9, the measured frequencies indicate dominantly an acoustic natural mode of the duct with a constant He value around 0.25. Whereas the Str reduces from 0.5 to 0.2, following a power law behavior with increasing Re. This plot has to be observed together with their corresponding pressure amplitudes plots for a better interpretation of the measured LCO. Therefore, the measured pressure [Pa] and UV Photo multiplier tube (PMT) intensity [arbitrary units] amplitudes (a) and the phase delay between Mic 4 and Mic 3, positioned across the wedge and between the *UV-PMT* and Mic 4 (b), are plotted in Figure 10. The amplitude plot clearly shows a low amplitude regime, transforming rather sharply around

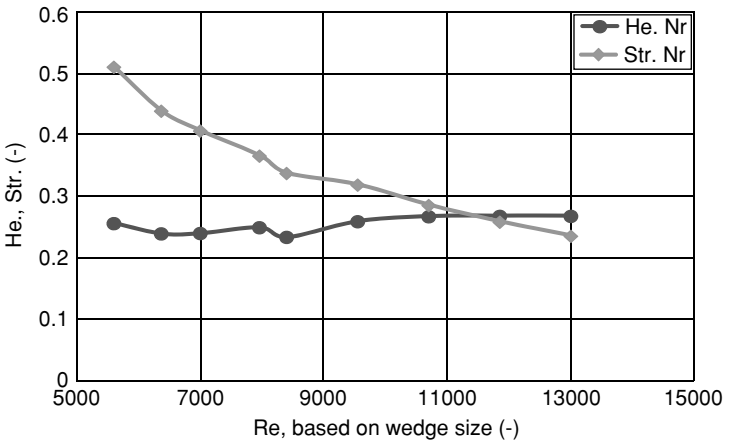

Figure 9: Measured peak frequencies as a function of flow rates, represented in terms of non-dimensional number such as Helmholtz (He), Strouhal (Str) and Reynolds (Re) numbers respectively.

Re = 9000 into a high amplitude regime. The amplitude of the *UV-PMT* intensity oscillations is considered to be directly proportional to the heat release rate fluctuations amplitude and is observed to show also a strong correlation with the pressure fluctuations during the LCO. The constant phase delay between the Mic 4 and Mic 3 around zero value indicates a continuity of the pressure field across the wedge and flame and without any acoustic losses. An interesting observation is that the phase delay between the *UV-PMT* and *Mic 4* reveals the relation between the heat release rate fluctuations and the pressure oscillations. A clear shift in phase delay values by 90 degrees can be observed at the separation of two regimes of high and low amplitude LCO. In the investigation performed by Chakravarthy et al. [9], they observed behavior of nearly constant *He* transitioning to a linearly increasing trend (which is equivalent to a hyperbolic trend in *Str* asymptoting to a constant value) and then a corresponding nonlinear increase in the amplitudes with increasing *Re,* which they referred as flow-acoustic lock on. They also observed a flow/geometric regime giving a constant *He* and *Str* varying hyperbolically, but without reaching a constant value indicating the absence of flow–acoustic lock on. In the current investigation, the second process is applicable, where the flow-acoustic lock on is not promoted as is indicated by the fact that the *Str* number does not reach a constant value. An additional investigation by phase locked CCD imaging with that of the pressure signal might be helpful to confirm the above analysis.

3.3. Influence of wall vibration on LCO:

The response of the combustor wall vibrations is measured using a Laser Doppler Vibrometer (LDV). The LDV is a non-contact laser technique that uses the Doppler shift of the laser beam frequency due to the motion of the surface. The output of a LDV is a signal proportional to the wall normal velocity component (of the wall movement) along the

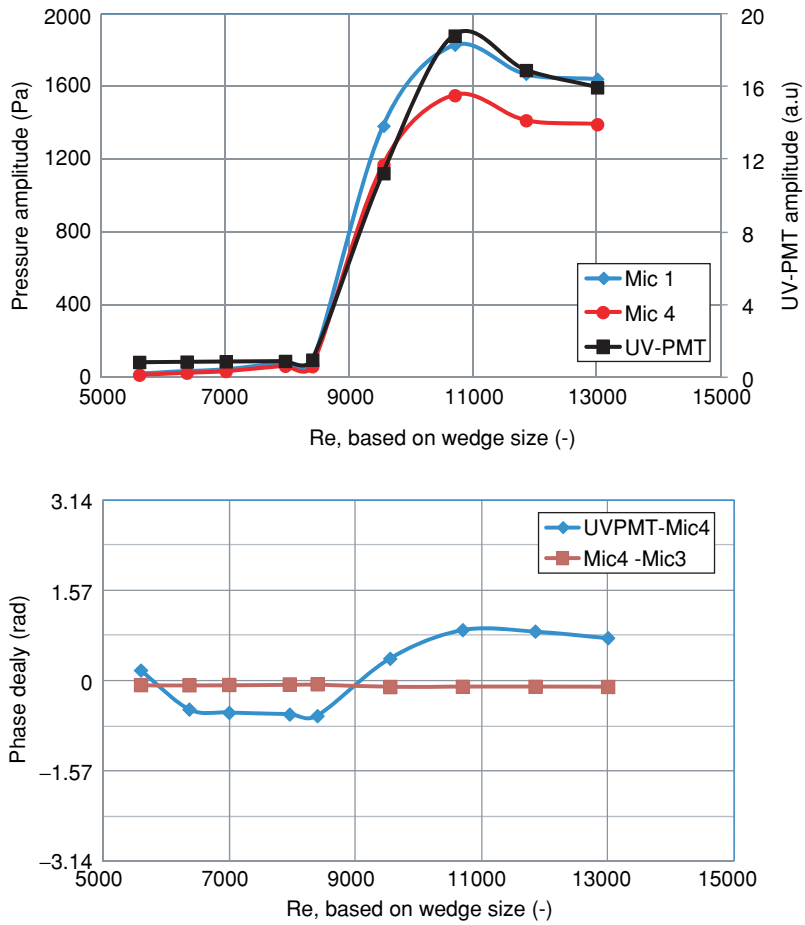

Figure 10: Measured peak pressure, *UV-PMT* intensity amplitudes (a) and phase delay between microphones 4–3 and *UV-PMT* - Mic 4 (b) as a function of flow rates characterized by Reynolds number Re.

direction of the laser beam. This technique is very useful in surfaces that are too hot to place a conventional accelerometer. The LDV signal was measured simultaneously with other dynamic pressure and chemiluminescence signals and stored on to a PC. For every operating condition, 8192 simultaneous samples were recorded for each channel at 2560 Hz.

In contrast with the earlier work presented by the authors [28], the effect of fluid structure interaction on the LCO behavior is negligible in this configuration with 4 mm wall thickness. It was shown in earlier work, with wall thickness 1 mm, that the LCO peak frequency was very much dictated by the structural Eigen frequency (which was around 100 Hz). The present (single and double liner) configuration with 4 mm wall thickness has a higher stiffness and thus has higher structural Eigen frequencies around 590 Hz. However, to give some more insight and appreciate the 2-way FSI, LDV

measurements were made at slightly different geometry (Vr3 combustor) and operating point and are shown in Figure 11. The x-axis has been normalized and represented as Helmholtz number ($He = f\ c/L$) to be able to compare different operating points and

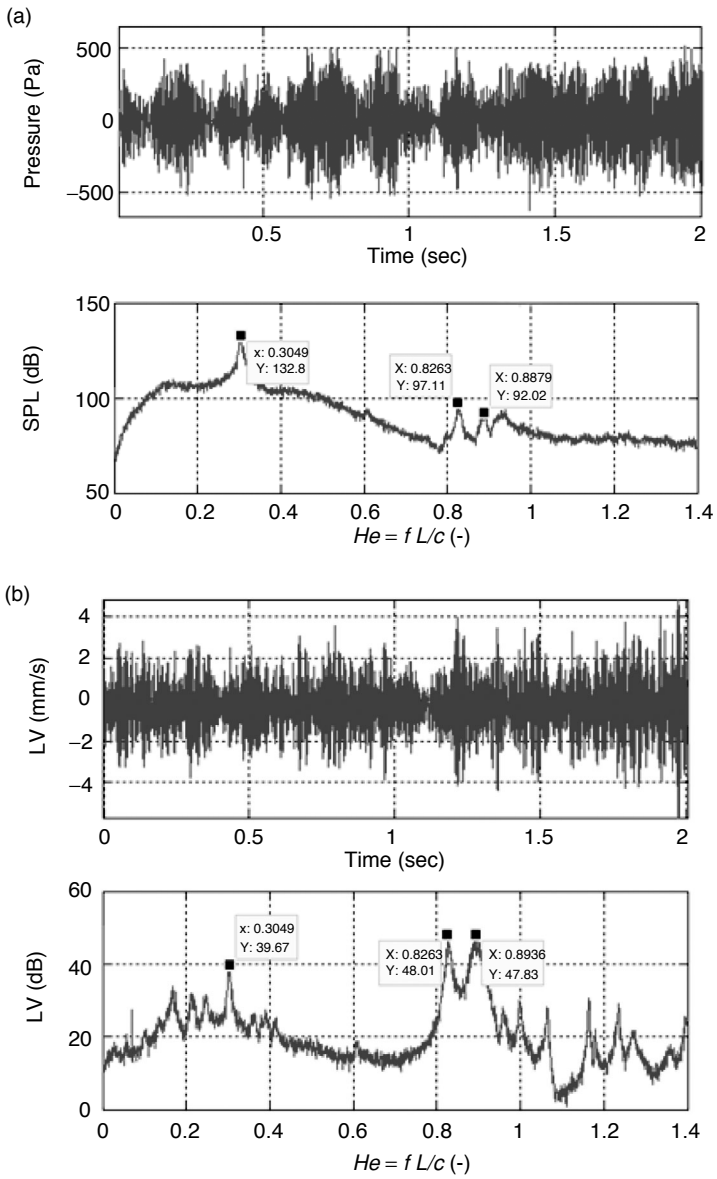

Figure 11: The time domain and the auto spectrum [dB] of the measured pressure (a) and wall vibration (b) at 60 kW and and $\lambda = 1.40$ in a slightly different combustor configuration.

Table 2: The results from the FEM modal analysis of the downstream duct (liner)

Mode no.	1	2	3	4	5
Freq. [Hz]	454	634	652	693	712
Freq. normalized, *He* [–]	0.59	0.82	0.85	0.9	0.92

configurations and with the numerical simulations. The pressure measurements (top) show the highest amplitude around *He* = 0.3 (~200 Hz) which is around the first acoustic Eigen mode of the combustor (fluid domain). Whereas, the simultaneously measured wall vibrations (bottom) with LDV show the larger amplitudes around He = 0.82, 0.89 which are close to the structural 2nd and 4th structural Eigen modes i.e., 634 Hz, 693 Hz respectively. To support this argument, a FEM modal analysis for the downstream duct (liner, L = 0.78 m) has been carried out in order to explain the peak frequencies measured using the laser vibrometer. The results are shown in Table 2. As discussed, the liner (structure) gains the energy from the LCO in the fluid domain and oscillates more intensively at one of its natural modes. It's not clear, yet, why the 2nd and 4th Eigen modes were excited rather than the first Eigen mode. In addition some small peaks can be observed in both the plots (see, Figure 11) other than their respective Eigen frequencies. This implies that the structure vibrates at its natural mode by taking the energy from the acoustic mode (LCO) and thus the relative amplitude differences at respective modes can be observed from the plot. With these experimental findings, it is not clear if the wall interaction has a positive or negative influence on the amplitude of the LCO.

3.4. Numerical simulations

First, the numerical simulation results from the fluid domain will be discussed. The pressure signal for the 40 kW and 60 kW cases, presented in the time domain [Pa] and as the auto spectrum [SPL, dB], as studied in the experiments has been plotted in Figure 12 and Figure 13. In Figure 12, the development of small scale pressure fluctuations into high, but finite, amplitude LCO is shown to be well predicted by the transient simulation at both 40 kW (top) and 60 kW (bottom) cases. The spectrum of the measured and simulated pressure is plotted together in Figure 13. To compare the simulations with the experiments that are performed at several operating points and combustor configurations (L = 1 m), the independent variable (frequency) at the x-axis has been normalized and represented as a Helmholtz number ($He = f\,c/L$). In both 40 kW and 60 kW cases the same value of average sound speed 'c = 770 m/s' is being used. This is because, theoretically the sound speed is strictly a function of temperature and is assumed to be constant for a given air factor (λ = 1.60) with more or less constant heat lossees.

By comparing the SPL plots with the experiments, the 40 kW case shows a larger over prediction of the amplitude than the 60 kW case. As pointed out previously [29], the inlet acoustic boundary condition (Ref. Coef, R) during the LCO is slightly

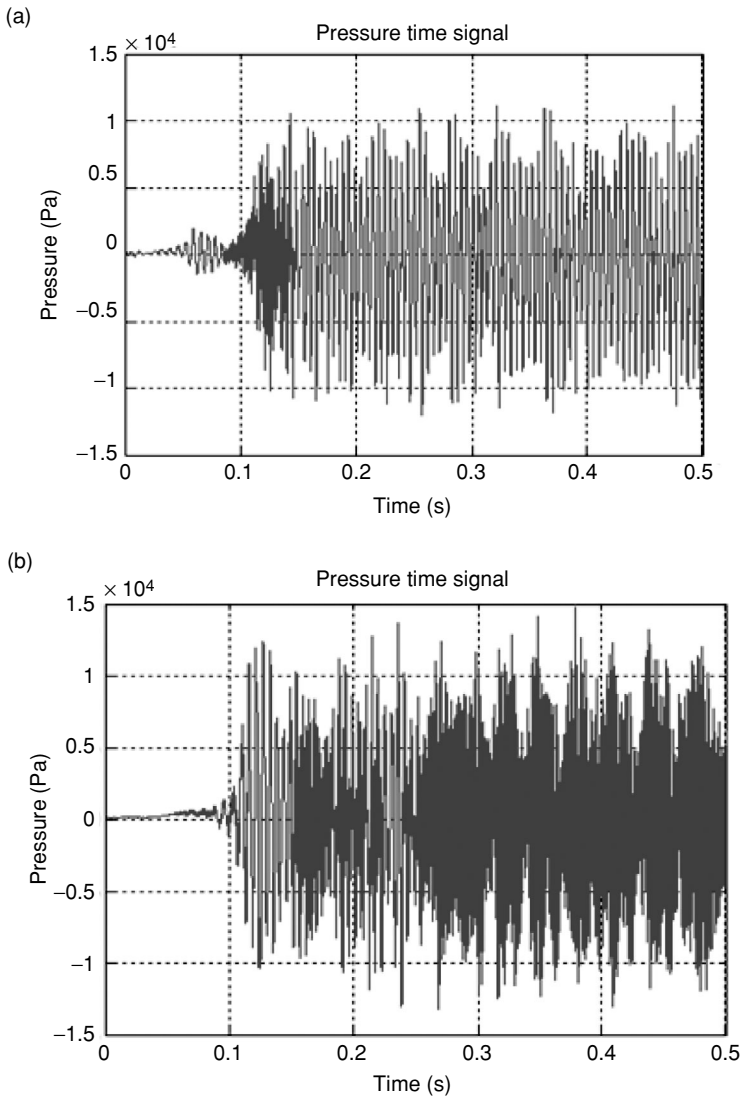

Figure 12: Simulated time domain [Pa] of the pressure signal at 40 kW (a) and 60 kW (b) at $\lambda = 1.60$.

dependent on the mean flow rates as well and shows an increasing trend with increasing mean mass flow rates or Reynolds number. Thus, the amplitude of the measured LCO might increase with increase in the mass flow rate and hence of the reflection coefficient (R). Whereas in the numerical simulation, due to a constant specified BC, this effect is not well captured and hence the over prediction in the 40 kW case is higher than the

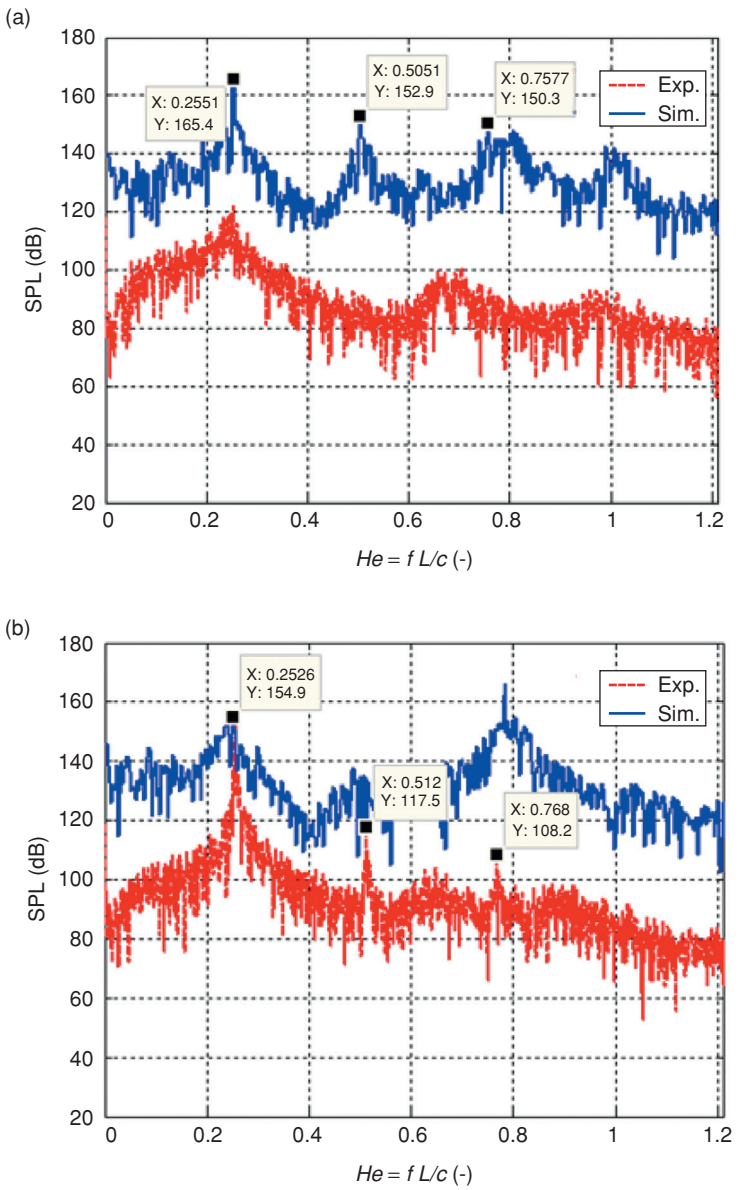

Figure 13: Comparison of the auto spectrum [SPL, dB] of the pressure signal at 40 kW (a) and 60 kW (b) at $\lambda = 1.60$ respectively.

60 kW case. However, the first and higher harmonics due to non-linear effects are well captured by the simulations, in particular for the 60 kW case. It is observed that the predicted acoustic time scales related to the geometry configuration and their resulting

natural modes are scaling well with the *He* number. The first mode Eigen frequency is observed around the characteristic *He* number of 0.255 for both the cases and their multiples at 0.51 and 0.76 are also very well captured. The model performance can be further improved by bringing additional damping into the system by means of a more advanced damping model or/and correct representation on the inlet acoustic boundary condition (R). On the other hand, it should be noted that this 2D simulation (2 mm slice) is still only an approximation of the whole 3D geometry, so the 2D approximation might also have the effect of less damping by having less turbulence-acoustics interaction.

Quantitatively the simulation results show an over prediction of the amplitude by an order of magnitude as compared to measured values. There are two reasons for this: First, the damping (either from the thermo viscous effects or structural wall vibrations) in the system is not yet modelled sufficiently accurately. Secondly, the boundary conditions in the CFD are strictly specified as constant values, whereas in reality the end conditions, especially at the inlet, change with operating conditions.

In a different study involving the same combustor, it was found that the reflection coefficient at the exits acts as a low pass filter having a value less than 1 at lower frequencies and closer to 1 at higher frequencies. With the CFD solver presently available in CFX, this kind of varying acoustic boundary condition implementation is not possible. The peak pressure levels read from CFD results are an order of magnitude higher than experimental values. If the instability in the system is increased by considering the double liner configuration, the peak pressure values are much closer to CFD results (see figure 7). Thus it suggests that the damping mechanism in CFD has to be further verified, especially for low amplification rates, i.e. situations near neutral stability. The authors would however like to emphasise that the frequencies of instability have been captured even the non-linear part of the phenomenon which is also an important concern of the study.

3.4.1. Numerical simulation of fluid structure interaction

As these simulations were made with coupled fluid structure interaction (FSI), it is possible to get the wall displacement spectrum, similar to the pressure spectrum, at a nodal point at the fluid-structure interface as shown in Figure 14. The time domain indicates measured wall displacement velocity amplitude up to ±2 mm/s. The frequency spectrum on the bottom side shows a few peaks, in the lower frequency domain, that was not present in the pressure spectrum. This can be attributed to the fact that the wall (structure) has dynamics at lower frequencies compared to that of the fluid domain. However, it can be seen that the peaks at *He* = 0.25 and 0.5 that are present in the pressure spectrum are observed also in the wall vibration spectrum, indicating a strong fluid structure interaction around the natural modes of the combustor (fluid domain). But, care should be taken while interpreting these results, as this simulation has been made with only 2D, 2 mm slice and may be over predicting the displacement amplitudes. When taking into account the full 3D wall structure the system becomes stiffer, the displacement magnitude can be lowered and the frequencies can go up as observed with Laser vibrometer measurements shown in Figure 11.

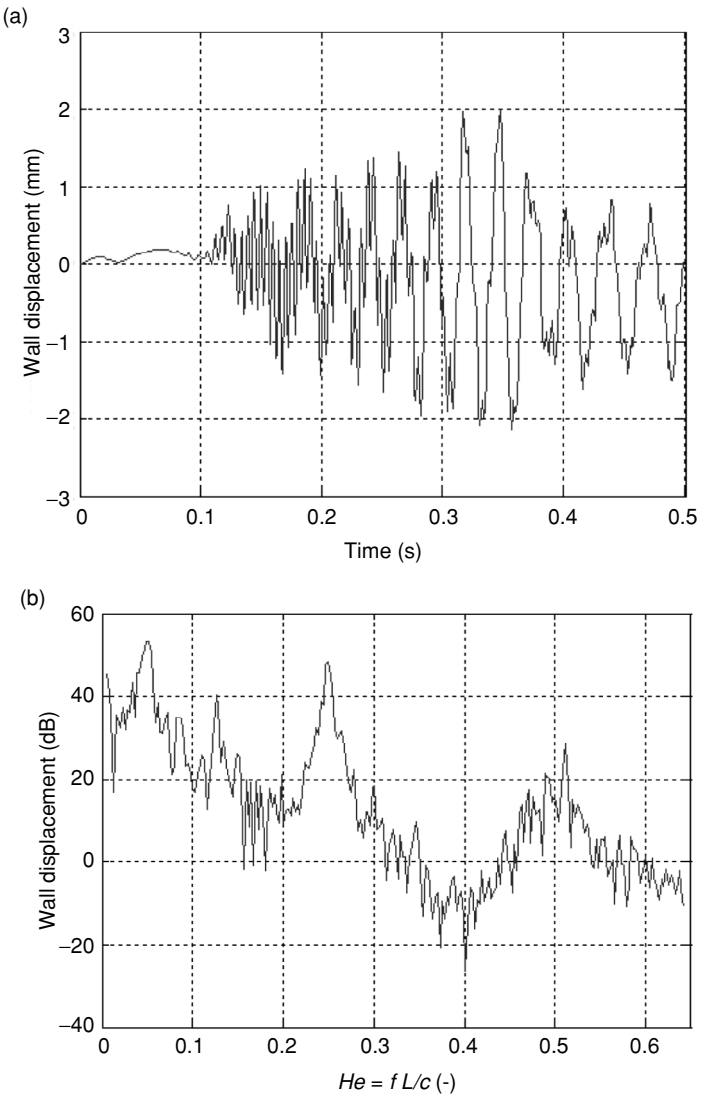

Figure 14: Time domain [mm] (a) and auto spectrum [dB] (b) of the simulated wall displacement amplitude for the case of 60 kW and $\lambda = 1.60$.

The simulation data were stored at a lower frequency (only each 10th time step) and thus the higher order effects cannot be obtained. The model can in the future be improved at the following points to allow a more direct experimental validation:

- Extend the 2D model to full 3D model
- Higher temporal resolution of the data saving may be every time step.

- Appropriate heat transfer effects (heat losses)
- Implementing the measured reflection coefficient/impedance in to the model, along with damping models/mechanisms.

5. CONCLUSIONS

In this work, a variation of the Rijke tube combustor geometry, with vibrating walls, has been investigated both experimentally and numerically in limit cycle operation. Numerically 2-way FSI modeling was applied. The measurements clearly indicated the characteristic frequencies of the LCO to be close to $He = 0.25$ and their higher harmonics due to non-linear effects. To differentiate between the mechanisms/processes responsible for the LCO, dimensionless numbers Strouhal (vortex shedding process) and Helmholtz number (duct acoustic processes) were plotted as a function of flow rate Reynolds number *Re*. Thus with the observed constant *He* the results indicate the observed dominant oscillation frequencies are associated with the acoustic modes of the combustor. There were also a few peaks around $He = 0.8$, which correspond to the structural natural modes of the combustor. The 2-way FSI simulations captured the presence of high amplitude pressure oscillations with peak frequencies around the first and higher order modes of the combustor correctly. However, the wall displacement results indicated a stronger presence of dynamics in the low frequency domain ($f < 100$Hz) instead of at higher frequencies as observed in the fluid domain. In future research it is expected that an improved model taking into account the 3D effects and the complete structure will provide more accurate predictions. Overall, the simulations compared with the experiments show a very good consistency. In particular, the peak frequencies around the natural modes and also the intermediate peaks due to non-linear effects have been reproduced quite satisfactorily. This gives the opportunity of the used URANS model (ANSYS commercial code) to explore the influence of limit cycle behavior on the structure and can be further developed to predict the life time of the gas turbine liner material.

ACKNOWLEDGEMENTS

This work is funded by the EC Marie Curie Action Initial Training Network program in project LIMOUSINE, grant application number 214905. The authors used ANSYS V13 for their simulations and thank Dr. Phil Stopford of ANSYS for his support.

REFERENCES

[1] Correa, S. M., *A Review of NOX formation under gas turbine combustion conditions,* Combust. Sci. and Tech., 1992, 87, 329–362.

[2] Lefebvre, A. H., *Gas Turbine Combustion*. [ed.] N. Chigier., McGraw-Hill, 1983.

[3] Keller, J. J., *Thermoacoustic Oscillations in Combustion Chambers of Gas Turbines*. 12, AIAA Journal, 1995, 33, 2280–2287.

[4] Lieuwen, T. and Yang, V., [ed.] *Combustion Instabilities in Gas Turbine Engines: Operational Experience, Fundamental Mechanisms and Modeling*. *ISBN 15637669X, In Prog*. *Astronotics and Aeronautics,* AIAA, 2006, 210.

[5] Poinsot, T. J., Trouve, A. C., Veynante, D. P., Candel, S. M. and Esposito, E. J., *Vortex-Driven Acoustically Coupled Combustion Instabilities*, J. Fluid Mech., 1987, 177, 265–292.

[6] Schadow, K. C. and Gutmark, E, *Combustion Instability Related to Vortex Shedding in Dump Combustors and Their Passive Control*, Prog. Energy Combust. Sci., 1992, 18, 117–132.

[7] McManus, K. R., Poinsot, T. and Candel, S. M., A review of active control of combustion instabilities. *Prog. Energy Combust. Sci.*, 1993, 19, 1–29.

[8] Lieuwen, T.; Torres, H.; Johnson, C. & Zinn, B. T., *A Mechanism of Combustion Instability in Lean Premixed Gas Turbine Combustors,* 99-GT-3, ASME, Indianapolis, Indiana, June 7–10, 1999.

[9] Chakravarthy, S. R., Shreenivasan, O. J., Boehm, B., Dreizler, A. and Janicka, J., *Experimental characterization of onset of acoustic instability in a non-premixed half-dump combustor*, J. Acoust. Soc. Am., 2007, 122 (1), 120–127.

[10] Fureby, C., *A computational study of combustion instabilities due to vortex shedding*, Proc. of the Combustion Institute, 2000, 28, 783–79.

[11] Fureby, C., Lofstorm, C., *Large-Eddy Simulation of bluff body stabilized flames*, 25th Symposium on Combustion, The Combustion Institute, 1994, 1257–1264.

[12] Karthik, B., Chakravarthy, S. R. and Sujith, R. I., *Mechanism of pipe-tone excitation by flow through an orifice in a duct*, J. Aero acoustics, 2008, 7 (3) 321–348.

[13] Mariappan, S. and Sujith, R. I., *Thermoacoustic instability in a solid rocket motor: non-normality and nonlinear instabilities, J. Fluid Mechanics,* 2010, 653*,* 1–33.

[14] Sujith, R. I, Non-normality and Nonlinearity in thermoacoustic instabilities, *Proc. of the 13th Asian Congress of fluid Mechanics,* Dhaka, Bangladesh, 17–21 Dec, 2010.

[15] Santosh Kumar, T.V, Alemela, P. R. and Kok, J. B. W., *Dynamics of flame stabilized by triangular bluff body in partially premixed methane-air combustor*, Proc. of ASME Turbo Expo 20011, Nr. GT2011-46241, Vancouver, Canada, 2011.

[16] Tinga, T., et al.. *Gas Turbine Combustor Liner Life Assessment Using a Combined Fluid/Structural Approach,* J. of Engg. for Gas Turbines and Power, 2007, 129, 69–79.

[17] Pozarlik, A. and Kok, J B W., *Numerical prediction of interaction between combustion, acoustics and vibration in gas turbines*: Acoustics 08, Paris, 2008, 2749–2754.

[18] Huls, R. "Acousto-elastic interaction in combustion chambers" PhD thesis, Universtiy of Twente, Enschede, Netherlands, 2006.

[19] Alemela, P. R., Juan Carlos Roman Casado, Santosh Kumar and Jim Kok, "Simulation of Limit Cycle Pressure Oscillations with Coupled Fluid-Structure Interactions in a model combustor", *18th Int. congress on sound and vibration*, Rio de Janeiro, Brazil, 10–14th July, 2011.

[20] Raun, R. L.; Beckstead, M. W.; Finlinson, J. C. & Brooks, K. P. A review of Rijke tubes, Rijke burners and related devices *Prog. Energy Combust. Sci.,* 1993, *19*, 313–364.

[21] Casado, J. C. R., Alemela, P. R., Ignacio Hernández Vera and Kok, J. B. W., "Experimental and numerical study of the effect of acoustic time delays on combustion stability", *18th Int. congress on sound and vibration*, Rio de Janeiro, Brazil, 10–14th July, 2011.

[22] Abom. A note on the experimental determination on acoustical two-port matricies. *J. of Sound and Vibration*, 1992, 155 (1), 185–188.

[23] Alemela, P.R., Fanaca, D., Ettner, F., Hirsch, C., Sattelmayer, T. and Schuermans, B., Flame transfer matrices of a premixed flame and a global check with modelling and experiments. GT2008-50111 in *Proc. of ASME Turbo Expo 2008*, Berlin, Germany, 2008.

[24] Kühlsheimer, C. and Büchner, H., Combustion dynamics of turbulentswirling flames. *Combust. and Flame*, 2002, 131, 70–84.

[25] Alemela, P. R., Fanaca, D., Hirsch, C., Sattelmayer, T. and Schuermans, B., "Determination and Scaling of Thermo-acoustic Characteristics of Premixed Flames", *Int. Journal of spray and combustion dynamics*, 2010, 2(2), 169–198.

[26] *DOWLING, A. P. "Nonlinear self-excited oscillations of a ducted flame", J. Fluid Mech.,* 1997, 346, 271–290.

[27] Kok, J. B. W. and Jager, Bram de. "The acoustic wave propagation equation in a turbulent combustion flow", : 14th ICSV, Cairns, Australia, 2007.

[28] Casado, J. C. R., Alemela, P. R. and Kok, J. B. W. "Combustion Dynamics coupled to Structural Vibration", *17th Int. congress on sound and vibration*, Cairo, Egypt, 18–22 July, 2010.

[29] Lamraoui, A., Richecoeur, F., Ducruix, S. and Schuller, T., Experimental analysis of simultaneous non-harmonically related unstable modes in a swirled combustor, Proc. of ASME Turbo Expo 2011, Nr. GT2011-46701, 2011, Vancouver, Canada, 2011.